

Magnetic bubble refraction and quasibreathers in inhomogeneous antiferromagnets

J.M. Speight

School of Mathematics, University of Leeds, Leeds LS2 9JT, UK

Abstract

The dynamics of magnetic bubble solitons in a two-dimensional isotropic antiferromagnetic spin lattice is studied, in the case where the exchange integral $J(\mathbf{x};\mathbf{y})$ is position dependent. In the near continuum regime, this system is described by the relativistic $O(3)$ sigma model on a spacetime with a spatially inhomogeneous metric, determined by J . The geodesic approximation is used to describe low energy soliton dynamics in this system: n -soliton motion is approximated by geodesic motion in the moduli space M_n of static n -solitons, equipped with the L^2 metric. Explicit formulae for various natural choices of $J(\mathbf{x};\mathbf{y})$ are obtained. From these it is shown that single soliton trajectories experience refraction, with J^{-1} analogous to the refractive index, and that this refraction effect allows the construction of simple bubble lenses and bubble guides. The case where J has a disk inhomogeneity (taking the value J_+ outside a disk, and $J_- < J_+$ inside) is considered in detail. It is argued that, for sufficiently large $J_+ = J_-$ this type of antiferromagnet supports approximate quasibreathers: two or more coincident bubbles confined within the disk which spin internally while their shape undergoes periodic oscillations with a generically incommensurate period.

1 Introduction

The purpose of this paper is to analyze the dynamics of bubble-like topological solitons arising in a two-dimensional classical Heisenberg antiferromagnet where the exchange interaction is isotropic, but not homogeneous. At each site $(i;j) \in \mathbb{Z}^2$ in a square lattice, one has a classical spin vector $S_{ij} \in \mathbb{R}^3$, with $\|S_{ij}\|^2 = s^2$, evolving according to the law

$$\frac{dS_{ij}}{dt} = -S_{ij} \times \frac{\partial H}{\partial S_{ij}}; \quad H = \sum_{i,j} J_{ij} (2s^2 + S_{ij} \cdot (S_{i,j+1} + S_{i+1,j})) \quad (1)$$

where t is time and J_{ij} are positive constants. This is the usual planar isotropic Heisenberg antiferromagnet, but in the case that the exchange integral J has been made inhomogeneous, that is, position dependent. The experimental means of achieving this J -inhomogeneity is left unspecified. One (perhaps naive) suggestion is that a sample of one antiferromagnetic material could be enriched, in places, with atoms from a different antiferromagnetic species. Note that since $J_{ij} > 0$ for all $i;j$, H is minimized when each spin anti-aligns with its nearest neighbours, just as in the homogeneous case.

It has been known for many years [1] that the dynamics of the homogeneous spin lattice ($J_{ij} = J > 0$, constant) is described in the continuum limit by the $O(3)$ nonlinear sigma model. In [2] it was shown, by adapting the dimerization process of Komineas and Papanicolaou [3], that this result generalizes in a natural way to the inhomogeneous problem considered here. That is, the continuum limit of system (1) is described by the nonlinear PDE

$$n \cdot Dn = 0; \quad Dn = \frac{\partial^2 n}{\partial t^2} - J(\mathbf{x};\mathbf{y})^2 \left(\frac{\partial^2 n}{\partial x^2} + \frac{\partial^2 n}{\partial y^2} \right) \quad (2)$$

where $n : \mathbb{R}^{2+1} \rightarrow \mathbb{R}^3$ has $\|n\| = 1$, t is a rescaled time variable, and $J(\mathbf{x};\mathbf{y})$ is a continuum approximant of J_{ij} . The relationship between n and S_{ij} is subtle. If we choose a lattice spacing $a > 0$, assumed small, then the

spin dynamics associated with a solution $n(t; x; y)$ of (2) is

$$S_{ij}(t) = (-1)^{i+j} s_n(2^{-\frac{1}{2}} s''; i''; j'') + O(s'') \quad (3)$$

Roughly speaking, one should imagine the field n sampled on a square lattice of spacing s'' , partitioned into black and white sublattices, chess-board fashion. The white spins evolve as $s_n(t)$, the black as $-s_n(t)$, where $t = 2^{-\frac{1}{2}} s''$.

Equation (2) is still the field equation of the nonlinear $O(3)$ sigma model on R^{2+1} , but now spacetime is equipped with a spatially inhomogeneous Lorentzian metric,

$$ds^2 = dt^2 - \frac{1}{J(x; y)^2} (dx^2 + dy^2) \quad (4)$$

Note that the static field equation is independent of J , so the usual Belavin-Polyakov lumps of the homogeneous system [4], which we shall call bubbles in this context (in analogy with magnetic bubbles in ferromagnets), carry over unchanged to the inhomogeneous system. Given the relativistic nature of (2), one can instantaneously boost these static bubbles to obtain moving bubble solutions. However, due to the inhomogeneity of J , such bubbles do not necessarily travel along straight lines. A detailed study of the trajectory of a single bubble interacting with various J -inhomogeneities was presented in [2]. The main conclusion is that, under most circumstances, bubble trajectories experience refraction, in analogy with geometric optics, $J(x; y)^{-1}$ playing the role of the refractive index of the medium. The incident and exit angles of a bubble crossing a domain wall J -inhomogeneity, for example, are related by Snell's law, and total internal reflection occurs if the impact is sufficiently oblique.

In the current paper, we shall briefly review this key refraction phenomenon, then go on to study some new dynamical problems which were not considered in [2]. Bubble refraction can be derived using only conservation laws and the assumption that the scattering of a bubble from a domain wall is approximately elastic [2]. However, in this paper our discussion of bubble dynamics will be entirely within the geodesic (or adiabatic) approximation of Manton [5], the standard approach to low-energy soliton dynamics in field theories of this type. The geodesic approximation, as applied to slow bubble dynamics, is set up in section 2. This framework is then used in section 3 to study the interaction of a single bubble with domain wall, trough and disk J -inhomogeneities. Finally the rotationally equivariant dynamics of n coincident bubbles in a disk J -inhomogeneity is studied in section 4. Here a dynamical phenomenon entirely absent from the homogeneous model, and with no optical analogue, is found. A charge n bubble set spinning about its symmetry axis can, in some circumstances, undergo periodic shape oscillations. These (approximate) solutions are spatially localized and, since the period of the shape oscillation need not be commensurate with the internal rotation period, in general, quasiperiodic in time. Hence they are quasibreathers. By contrast, a charge n bubble set spinning in the homogeneous model simply spreads out indefinitely. The inhomogeneity of J may thus act to stabilize spinning bubbles.

2 The geodesic approximation

Equation (2) is the variational equation for the action

$$S = \frac{1}{2} \int dt dx dy \left(\dot{n}^2 - \frac{1}{J(x; y)^2} (\nabla n)^2 \right) = \int dt (T - V) \quad (5)$$

where

$$T = \frac{1}{2} \int dx dy \frac{1}{J(x; y)^2} \left(\frac{\partial n}{\partial t} \right)^2; \quad V = \frac{1}{2} \int dx dy \left(\frac{\partial n}{\partial x} \right)^2 + \left(\frac{\partial n}{\partial y} \right)^2 \quad (6)$$

are identified as the kinetic and potential energy functionals respectively. Note that while T depends on J , V does not. This is a consequence of the deep fact that the sigma model potential energy (often called the harmonic or Dirichlet energy) on a space of dimension 2 depends only on the conformal class of the spatial metric. In our problem this metric is $g = J(x; y)^{-2} (dx^2 + dy^2)$ which is conformal to the Euclidean metric for

any choice of $J(x; y)$. It follows that Belavin's and Polyakov's analysis of the static homogeneous model [4] carries over unchanged to the inhomogeneous system. There is a topological lower energy bound

$$V[n] \geq 4\pi n \quad (7)$$

n being the topological degree of the map $n: \mathbb{R}^2 \rightarrow \mathbb{CP}^1 \cong S^2$. It is useful to define complex coordinates $z = x + iy$ on the spatial plane and $u = (n_1 + in_2)/(1 - n_3)$ on the target sphere (the latter being the image of n under stereographic projection from $(0; 0; 1)$ to the equatorial plane). Then the bound (7) for $n \neq 0$ is attained if and only if $u(z)$ is a rational map of algebraic degree n , that is

$$u(z) = \frac{a_0 + a_1 z + \dots + a_n z^n}{b_0 + b_1 z + \dots + b_n z^n} \quad (8)$$

where a_i, b_i are complex constants, at least one of a_n, b_n is nonzero, and the numerator and denominator share no common roots. Since such maps minimize V globally within their homotopy class, they are automatically stable static solutions of the model.

Without loss of generality we may choose the boundary value of n at spatial infinity to be $(0; 0; 1)$, that is $u(\infty) = 1$, so that $b_n = 0$ and hence $a_n \neq 0$. Since $a_n \neq 0$, we may divide the numerator and denominator by a_n and relabel $a_i = a_n^{-1} a_i, b_i = b_n^{-1} b_i$, so that the general static solution is

$$u(z) = \frac{a_0 + a_1 z + \dots + a_{n-1} z^{n-1} + z^n}{b_0 + b_1 z + \dots + b_{n-1} z^{n-1}} \quad (9)$$

This is uniquely specified by the $2n$ complex constants a_0, \dots, b_{n-1} . Hence the moduli space (or parameter space) of degree n static solutions, M_n , may be identified with an open subset of \mathbb{C}^{2n} , namely the complement of the complex codimension 1 algebraic variety on which the numerator and denominator have common roots. For example, the general degree 1 bubble is

$$u(z) = e^{i\theta} (z - w); \quad (10)$$

$\theta \in [0; 2\pi)$, $w \in \mathbb{C}$ and $w = w_1 + iw_2 \in \mathbb{C}$ being constants interpreted as the bubble's width, internal phase and position respectively. Hence M_1 is diffeomorphic to $\mathbb{C} \times \mathbb{C}$, where $\mathbb{C} = \mathbb{C} \setminus \{0\}$. In general M_n has real dimension $4n$, and may be thought of as the configuration space of n unit bubbles. However, it is not diffeomorphic to $(M_1)^n$, and its parameters cannot globally be identified with the positions, widths and orientations of n separate bubbles.

Following Ward [6] and Leese [7], we may study the low energy dynamics of n bubbles within the geodesic approximation of Manton [5]. The idea is that M_n , the $4n$ dimensional space of static degree n solutions, is the flat valley bottom in the space of all degree n maps $\mathbb{R}^2 \rightarrow S^2$, on which V attains its minimum value of $4\pi n$. Consider the Cauchy problem in which the constituent bubbles of a static n -bubble are set off in relative motion with small speeds. Then the initial field lies in M_n , the initial velocity field is tangential to M_n , and the system has only a small amount of kinetic energy. Hence its subsequent motion in field configuration space is confined close to M_n by conservation of energy $E = T + V$ (note that T is strictly positive). This suggests that a collective coordinate approximation wherein the motion is constrained to M_n for all time is sensible. This is often called an adiabatic approximation, since we assume that at each time the field configuration is well approximated by a static solution, but that the parameters in this solution may vary slowly with time.

Let q^1, \dots, q^{4n} be an arbitrary real coordinate system on M_n (for example, the real and imaginary parts of $a_0, \dots, a_{n-1}; b_0, \dots, b_{n-1}$), and let us denote by $u_0(z; q)$ the static n -bubble corresponding to $q = (q^1, \dots, q^{4n})$. Then the adiabatic approximation asserts that

$$u(z; t) = u_0(z; q(t)); \quad (11)$$

We now substitute (11) into S , and obtain variational equations for q . Note that $V = 4\pi n$, constant, for all fields of the form (11), and T is quadratic in time derivatives, so the action reduces to (Einstein summation convention applied)

$$S = \frac{1}{2} \int dt \left(\dot{q}^i \dot{q}^j g_{ij}(q) - 4\pi n \right); \quad g_{ij}(q) = \int \frac{dx dy}{J(x; y)^2} \frac{4}{(1 - |u_0(z; q)|^2)^2} \frac{\partial u_0}{\partial q^i} \frac{\partial u_0}{\partial q^j}; \quad (12)$$

This is the action for geodesic motion on M_n with respect to the metric $ds^2 = g_{ij}(q) dq^i dq^j$. Hence we expect $u(z;t)$ to be well approximated by geodesic motion in $(M_n; g)$, at least for low speeds. It should be emphasized that this does not mean that individual bubbles follow geodesics in physical space $(R^2; g)$, even in the case $n = 1$. Indeed, the motion of 2-bubbles even in Euclidean space (i.e. even in the homogeneous model) is highly nontrivial [6, 7]. For example, two identical bubbles head directly at one another do not pass through one another unchanged, or achieve some minimum separation then recede along their line of approach, as one might expect. Rather, they coalesce to form a ringlike coincident 2-bubble, then break apart and recede along a line perpendicular to their line of approach. This behaviour is generic to planar topological solitons in relativistic field theories, and is well-understood within the geodesic approximation [8]. The conceptual framework and validity of the geodesic approximation are discussed at length in [9].

The metric g , and hence the dynamics, depends strongly on $J(x; y)$. The main task in this approach to topological soliton dynamics is to calculate this metric. Even in the degree 1 case this is impossible to compute explicitly unless J takes a particularly simple, symmetric form. Nonetheless, much qualitative information about g can be deduced, and this can lead to a good understanding of the dynamics of a single bubble even in the absence of explicit formulae. In the case of higher degree, $n \geq 2$, the moduli space is too large for the general geodesic problem to be tractable, even if g is known explicitly. To make progress one must reduce the dimension by identifying totally geodesic submanifolds. This amounts to imposing symmetry constraints on the initial data.

The metric in the case $n = 1$ has a particularly simple form. If J is constant, we are studying the standard sigma model, and it is found that α and β are frozen by infinite inertia ($\dot{\alpha} = \dot{\beta} = 1$) and $\dot{w} = 4 J^{-2} dw/dt$, so bubbles just travel at constant velocity [6]. At the other extreme, if $J(x; y) = 1 + x^2 + y^2$, we effectively have the sigma model on a round two-sphere, and the bubble dynamics is much richer [10]. This choice has J unbounded, which is presumably unphysical, however. Assuming that J remains bounded, α and β are frozen by an essentially identical argument to Ward's. Without loss of generality, we can set $\alpha = 0$. The width w remains a free, but frozen, parameter. The metric on M_1 , the width w , phase 0 leaf of M_1 , is then

$$ds^2 = f(w) (dw_1^2 + dw_2^2); \quad (13)$$

where

$$f(w) = \frac{\int \frac{dz dz}{J(z; z)^2} \frac{4 - w^2}{(1 + w^2)^2} = \frac{\int \frac{4 du du}{(1 + |u|^2)^2} \frac{1}{J(u + w)^2}; \quad (14)$$

the integral of $J(u + w)^{-2}$ over the standard unit sphere on which u is a stereographic coordinate. Note that

$$\lim_{w \rightarrow 0} f(w) = \frac{4}{J(w)^2} (dw_1^2 + dw_2^2) = 4 g; \quad (15)$$

In the limit of vanishing bubble width, therefore, the trajectories of isolated bubbles tend to geodesics, not just in M_1 , but also in the physical plane. One may regard the metric g on M_1 as a smeared out version of g , due to the bubble's finite core size.

3 Bubble refraction

The simplest J -inhomogeneity of all is the domain wall. Let us assume that J depends only on x , is constant outside a small neighbourhood $(-\epsilon; \epsilon)$ of $x = 0$ and rises monotonically from J to J_+ as x traverses this neighbourhood. Such a $J(x)$ might arise from enriching one end of an antiferromagnet but not the other, for example. It follows immediately from (14) that the conformal factor $f(w)$ of the metric g on M_1 depends only on w_1 , is monotonically decreasing and has

$$\lim_{w_1 \rightarrow 1} f(w_1) = \frac{4}{J^2}; \quad (16)$$

Our analysis of the interaction of the bubble with the domain wall will use only these properties of f . An explicit formula for f can be obtained in the limit of vanishing domain wall width $\epsilon \rightarrow 0$. If we idealize the domain wall by a step function,

$$J(x) = \begin{cases} J_+ & x \geq 0 \\ J & x < 0 \end{cases}; \quad (17)$$

we find from (14), and some elementary spherical geometry [2], that

$$f(w_1) = \frac{2}{J^2} \left(1 - \sqrt{\frac{a_1}{2 + a_1^2}} \right) + \frac{2}{J_+^2} \left(1 + \sqrt{\frac{a_1}{2 + a_1^2}} \right) : \quad (18)$$

Note that f decreases smoothly from $4 = J^2$ to $4 = J_+^2$, as expected.

To analyze geodesic flow in M_1 , it is helpful to use the Hamiltonian formalism. The position coordinates w_1, w_2 have canonically conjugate momenta

$$p_1 = f(w_1)w_1; \quad p_2 = f(w_1)w_2; \quad (19)$$

and the flow is generated by the Hamiltonian

$$H = \frac{1}{2f(w_1)} (p_1^2 + p_2^2); \quad (20)$$

Both H and p_2 are integrals of the motion. Since geodesic trajectories are independent of initial speed, we may assume, without loss of generality, that $H = \frac{1}{2}$. Trajectories now fall into a one-parameter family labelled by the conserved momentum p_2 , which given (20) must satisfy $p_2^2 < \sup_{w_1 \in \mathbb{R}} f(w_1) = 4 = J^2$. The image of a momentum p_2 trajectory under projection to the (w_1, p_1) plane in phase space lies in the level set $f(w_1) - p_1^2 = p_2^2$. A sketch of these (projected) trajectories is presented in figure 1. They are confined to the bottle shaped region bounded by the curves $p_1 = \pm \sqrt{f(w_1)}$ whose union is the level set with $p_2^2 = 0$. These curves themselves correspond to a bubble hitting the domain wall with incidence angle 0 (i.e. orthogonal to the wall) and travelling straight through it, either left to right (upper curve) or right to left (lower). Two types of trajectory are evident. If $0 < p_2^2 < 4 = J_+^2$, then w_1 never vanishes and the bubble passes through the wall. We call these refracted trajectories. If $4 = J_+^2 < p_2^2 < 4 = J^2$, the trajectories have $\lim_{t \rightarrow \pm\infty} w_1(t) = \pm 1$, so the bubble approaches the wall from the left and is reflected by it. We call these reflected trajectories. Let $\theta(t)$ be the angle between the bubble's velocity and the x axis, so $\underline{w} = \underline{j} \sqrt{f(w_1)} \hat{e}^{i\theta(t)}$. Then

$$\sin \theta(t) = \sqrt{\frac{w_2}{w_1^2 + w_2^2}} = \sqrt{\frac{p_2}{p_1^2 + p_2^2}} = \sqrt{\frac{p_2}{f(w_1(t))}}; \quad (21)$$

Hence for a refracted trajectory incident on the domain wall from the left,

$$\frac{\sin \theta(1)}{\sin \theta(-1)} = \frac{f(-1)}{f(1)} = \frac{J_+^2}{J^2} \quad (22)$$

so the incident and exit angles of the trajectory, $\theta(-1)$ and $\theta(1)$, are related by Snell's law of refraction, with J^{-2} identified with the refractive index. If $\sin \theta(-1) > J = J_+$, then $p_2^2 > 4 = J_+^2$ and total internal reflection occurs.

It is interesting to make a similar qualitative analysis in the case of a straight trough J inhomogeneity. Assume that J is again independent of y , that $J(x) = J_1$ for $|x| \geq 1$, $J_1 > 0$, small; that $J(x) = J_2 < J_1$ for $|x| \leq 1$; and that J interpolates monotonically between the constant values J_1, J_2 in the narrow transition intervals $(1 - \epsilon; 1 + \epsilon)$ and $(-1 - \epsilon; -1 + \epsilon)$. Given Snell's law for domain walls [2], one expects this to be a bubble guide: we have an infinite strip in which the refractive index is $1/J_2$, greater than the refractive index $1/J_1$ in the surrounding region, so a bubble initially in and moving roughly along the strip should be trapped in the strip by total internal reflection, just as a light ray is confined within a fibre-optic cable.

The key point is, once more, to understand the conformal factor $f(w)$ of the metric on M_1 . Clearly f depends only on w_1 and tends to $4 = J_1^2$ as $w_1 \rightarrow \pm\infty$. In general, it is hump shaped, with a single critical point, a global maximum. If we assume $J(w_1)$ is even, then so is $f(w_1)$, and this maximum, which is always less than $4 = J_2^2$, occurs at $w_1 = 0$. Again, in the sharp wall limit, $\epsilon \rightarrow 0$, we can find an explicit expression for $f(w_1)$. The point is that $J(w_1)$ is piecewise constant in this limit, so from (14), we need only compute the area of the region on S^2 whose stereographic image is the vertical strip $-\epsilon < \operatorname{Re}(u + w) < \epsilon$. This is easily deduced from the sharp domain wall calculation in [2] (which led to formula (18)), yielding

$$f(w_1) = \frac{4}{J_1^2} + 2 \left(\frac{1}{J_2^2} - \frac{1}{J_1^2} \right) \sqrt{\frac{w_1 + 1}{(w_1 + 1)^2 + 1}} \sqrt{\frac{w_1 - 1}{(w_1 - 1)^2 + 1}} : \quad (23)$$

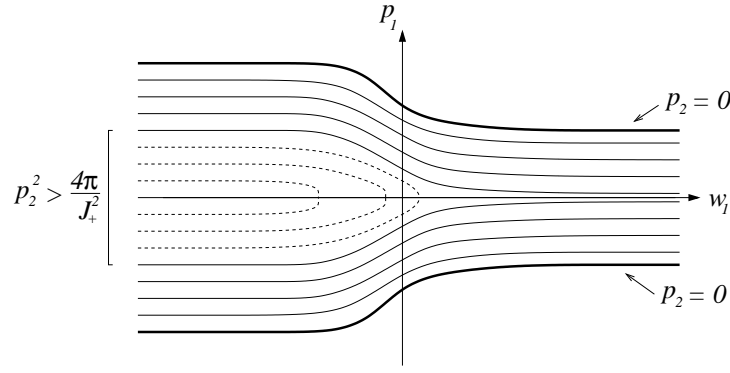


Figure 1: Projected phase portrait of the geodesic flow in M_1 for a domain wall J -inhomogeneity. The exchange integral on the right of the wall, J_+ , exceeds that on the left, J_- . Trajectories are bounded between the upper and lower bold curves, for which $p_2 = 0$. Dashed trajectories, which have $\frac{4}{J_+^2} < p_2^2 < \frac{4}{J_-^2}$, correspond to bubbles undergoing total internal reflection.

Note that this function has the qualitative features predicted.

The Hamiltonian discussion of geodesic flow in $(M_1; \cdot)$ is similar to the domain wall case. Once again we choose $H = \frac{1}{2}$ and sketch the level curves $f(w_1) = p_1^2 = p_2^2$ in the $(w_1; p_1)$ plane for $0 < p_2^2 < f_{\max} = f(0)$. Again, two regimes emerge separated by the case $p_2^2 = p^2 = 4/J_1^2$, see figure 2. For $p_2 < p$ the trajectories are unbounded and w_1 never vanishes. These correspond to a bubble hitting the trough from outside and passing right through it, being refracted twice in the process, so that its initial and final velocities coincide. For $p_2 > p$ the (projected) trajectories are bounded and periodic. These correspond to a bubble being directed along the direction of the trough by total internal reflection. The actual bubble trajectory in the physical plane is not periodic, of course, since it drifts uniformly in the y -direction (w_2 never vanishes; it is not constant, however). Note that even in this trapped regime, the bubble trajectory is not necessarily confined within the trough itself. Indeed, given any $R > 0$, there exists a trapped geodesic for which $\max_t |w_1(t)| > R$. In this sense, the behaviour of bubble trajectories is quite different from that of light rays in geometric optics.

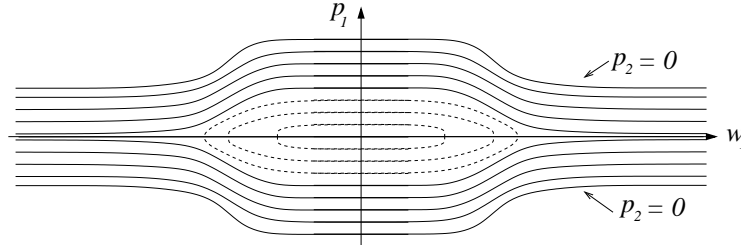


Figure 2: Projected phase portrait of the geodesic flow in M_1 for a trough J -inhomogeneity: the exchange integral is J_1 outside a vertical strip, within which it falls to $J_2 < J_1$. The closed dashed trajectories, which have $p_2^2 > \frac{4}{J_1^2}$, correspond to bubbles being guided along the trip by total internal reflection.

The bubble guidance effect does not depend on the trough being straight. The case of a circular trough (where the value of J is suppressed in an annulus) was considered in [2], the results being qualitatively similar.

Another interesting effect reminiscent of geometric optics is the phenomenon of bubble trajectory focussing by a circular "lens". Imagine J depends only on $|z|$ so that $J(|z|) = J_-$ for $|z| \leq 1$, $J(|z|) = J_+ > J_-$ for $|z| > 1$, interpolating smoothly and monotonically between these values in the narrow annulus $1 - \epsilon < |z| < 1 + \epsilon$. We have a disk where the refractive index $1/J_-$ exceeds that of the surrounding medium, so we expect single bubble trajectories to be refracted by this inhomogeneity like light rays passing through a circular lens. It follows immediately from (14) that the conformal factor in the metric depends only on $|w|$. In the sharp

will limit it to 0, it can be explicitly computed,

$$f(j) = \frac{2}{J^2} \left(1 - \frac{1}{\sqrt{4 + 2J^2(j^2 + 1) + (j^2 - 1)^2}} \right) + \frac{2}{J_+^2} \left(1 + \frac{1}{\sqrt{4 + 2J_+^2(j^2 + 1) + (j^2 - 1)^2}} \right) : \quad (24)$$

The geodesic problem in M_1 may easily be solved numerically, see figure 3. Note that parallel incident trajectories are approximately focussed by the lens, as expected.

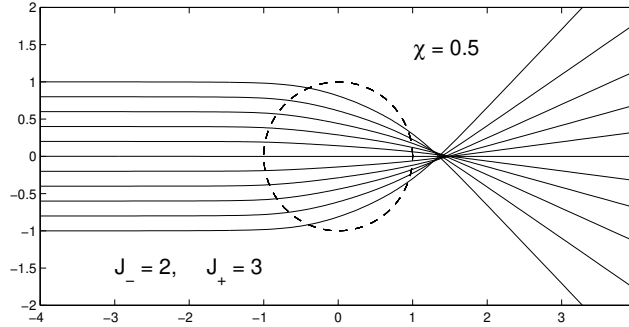


Figure 3: Focussing of parallel bubble trajectories by a disk J -inhomogeneity. The exchange integral is lower ($J_- = 2$) within the disk than in the surrounding plane ($J_+ = 3$).

4 Quasibreathers

All the J -inhomogeneities we have considered enjoy some kind of symmetry, either translational (domain walls and troughs) or rotational (disks). In this section, we will continue to impose rotational invariance, so $J = J(j)$. However, our emphasis will be very different: we will study rotationally equivariant n -bubble dynamics for $n \geq 2$. This corresponds to n coincident magnetic bubbles sitting, for all time, at the symmetry origin $z = 0$. This is dynamically interesting because for $n \geq 2$ the n -bubble width is no longer a frozen parameter. The n -bubble can spin internally and spread out or sharpen. So the dynamics of interest is no longer bubble transport, but rather the internal motion of the n -bubble. We will again model this within the geodesic approximation.

First note that, if $J = J(j)$, there is a natural isometric action of $U(1)$ on $(M_n; j)$, given by

$$u(z) \mapsto e^{ni} u(e^i z) : \quad (25)$$

The fixed point set of this action is necessarily a totally geodesic submanifold of $(M_n; j)$, which we shall call $(M_n^{\text{eq}}; j)$, where j is the induced metric. In fact [11], M_n^{eq} is, for all n , diffeomorphic to C^n , since it consists of the rational maps

$$u(z) = cz^n; \quad c \in C^n : \quad (26)$$

Since $U(1)$ equivariance is a valid symmetry reduction of the full field equation (2), one may regard geodesic flow in $(M_n^{\text{eq}}; j)$ either as a low energy approximation of the symmetry-reduced field equation, or as a symmetry reduction of the general geodesic approximation.

The geometry of M_n^{eq} is most easily understood by studying the lift of j to the n -fold cover \tilde{M}_n^{eq} of M_n^{eq} [11]. This is again diffeomorphic to C^n , and the covering projection is

$$\tilde{M}_n^{\text{eq}} \rightarrow M_n^{\text{eq}}; \quad (\tilde{z}) = z^n : \quad (27)$$

Hence, the n -bubble corresponding to $\tilde{z} \in C^n$ is $u(z) = (\tilde{z})^n$. Clearly any of the n points $e^{2\pi i k/n} \tilde{z}$ in \tilde{M}_n^{eq} , $k = 0, 1, \dots, n-1$, give the same n -bubble. We may think of j as the n -bubble width, and the argument

of ϕ , mod 2π , as being an internal phase. The potential energy density of an n -bubble is rotationally symmetric, vanishes at $z = 0$ and $|j| = 1$, and attains its maximum at

$$|j| = |j| \frac{n-1}{n+1} \frac{1}{z^n} : \quad (28)$$

The lifted metric on \mathbb{M}_n^{eq} is

$$e = f(|j|) d\bar{\sigma} ; \quad f(|j|) = 8 \int_0^{|j|} dr \frac{r^{2n+1}}{(1+r^{2n})^2 J(|j|)^2} : \quad (29)$$

In the homogeneous case, $J(|j|) = J_0$, constant, the metric is $e = C_n d\bar{\sigma}$ where C_n is a constant depending on n , so that $(\mathbb{M}_n^{\text{eq}}; e)$ is actually isometric to the Euclidean punctured plane, and the lifted geodesics are simply straight lines traversed at constant speed. It follows that all geodesics have $|j| = 1$ either as $t \rightarrow 1$ or as $t \rightarrow -1$, and, except in the case where $\phi(t)$ is a half ray hitting the missing point $\phi = 0$, both. The half rays correspond (when oriented inwards) to an n -bubble with no angular momentum collapsing to form a singularity in finite time. The straight lines missing $\phi = 0$ correspond to n -bubbles with angular momentum which spread out indefinitely as $|j| \rightarrow 1$. In total, each spin $n(z)$ in such a bubble executes $n=2$ complete rotations about the n_3 axis.

The behaviour is rather more interesting if we allow $J(|j|)$ to be non-constant. The "spherical" case $J(|j|) = 1 + |j|^2$ was studied in detail in [11]. One nice, and rather unexpected, fact in this case is that the volume of \mathbb{M}_n^{eq} , which turns out to be finite, is actually independent of n . One can isometrically embed \mathbb{M}_n^{eq} in \mathbb{R}^3 as a surface of revolution, and this surface has conical singularities of deficit angle $2(1-n^{-1})$ at $c = 0$ and $c = 1$. However, this case has J unbounded, which is not physically reasonable. We shall here consider the circular lens case, where J is suppressed in a disk centred on the origin. For simplicity, we will use the sharp wall limit, that is

$$J(|j|) = \begin{cases} J_+ & |j| > 1 \\ J & |j| \leq 1 \end{cases} \quad (30)$$

with $J_+ > J$. We saw in the last section that the metric on M_1 could be computed explicitly for this $J(|j|)$. We emphasize that this is not the metric of interest in the present context, however. Recall that position in M_1 is specified by the bubble's position in the physical plane, and the bubble width is a frozen parameter. By contrast, position in \mathbb{M}_n^{eq} is specified by the n -bubble's width and internal phase, and its location in the physical plane is fixed. In [2] an interesting bifurcation in the geodesic flow on M_1 was observed when ϕ is varied: as ϕ increases through a critical value, a pair of periodic geodesics appears in which the lump orbits in a circle centred on $z = 0$, one just inside the lens, one just outside. We will see that there is a geometrically similar bifurcation in the geodesic flow in \mathbb{M}_n^{eq} , but its physical meaning is now completely different, and the bifurcation parameter is $J_+ = J$, not the bubble width (now a dynamical variable).

Assuming J is given by (30), one sees that

$$f(|j|) = \frac{2-n^2}{J^2} \left(\frac{1}{n^2 \sin^2 \phi} - 1 \right) + \frac{J^2}{J_+^2} \int_0^{|j|} ds \frac{s^{n-2}}{(1+s^n)^2} : \quad (31)$$

Since the integrand is rational, one can, in principle, write down f explicitly for any choice of n . The expressions are not terribly enlightening however, even for small n , so we will omit them. More useful is the fact that, provided $J_+ = J$ is not too large, \mathbb{M}_n^{eq} can be isometrically embedded as a surface of revolution in \mathbb{R}^3 . Generating curves for these surfaces in the case $n = 2$, generated by the method described in [11], are depicted in figure 4. If $J_+ = J = 1$ the surface is just a (punctured) plane, swept out by rotating a straight half-line. As $J_+ = J$ increases, the generating curve becomes hump-shaped, until eventually, it forms a bulge above a narrower neck. At this point, a bifurcation in the geodesic flow occurs. A pair of periodic geodesics with $|j|$ constant appears, and there are quasiperiodic (and periodic) geodesics which remain confined within the bulge. These correspond to quasibreathers. As $J_+ = J$ increases further, the isometric embedding is lost, but the existence of quasibreather geodesics persists.

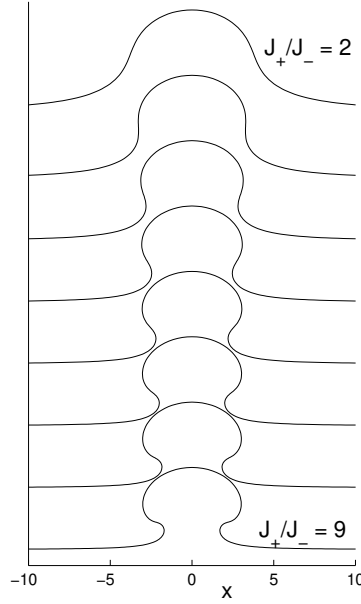


Figure 4: Generating curves for \mathbb{M}_2^{eq} isometrically embedded as a surface of revolution in \mathbb{R}^3 in the case of a sharp disk J -inhomogeneity with $J = J_+ = 2; 3; \dots; 9$ (top to bottom). The surfaces are swept out as these curves are rotated about the vertical axis $x = 0$. Note that a neck develops as $J_+ = J_-$ becomes large.

To confirm this visual reasoning, let us again consider the phase portrait of the geodesic flow. Introducing polar coordinates $(\theta; \dot{\theta})$ on \mathbb{M}_n^{eq} by $e^i = \frac{x^i}{r}$, the flow is generated by Hamiltonian

$$H = \frac{1}{2f(\theta)} \dot{\theta}^2 + \frac{p^2}{2}; \quad (32)$$

the conjugate momenta being

$$p_\theta = f(\theta)\dot{\theta}; \quad p_r = \dot{r} \sqrt{2f(\theta)}; \quad (33)$$

Both H and p_r are integrals of the motion, and we may choose $H = \frac{1}{2}$ without loss of generality. The trajectories, after projection to the $(\theta; p_\theta)$ halfplane (note $\dot{\theta} > 0$) are given by the level sets

$$2(f(\theta) - p_\theta^2) = p_r^2 \quad (34)$$

for $p_r^2 \in [0; 1]$. These level sets are plotted for $J_+ = J_- = 2$ and $J_+ = J_- = 4$ in the case $n = 2$ in figure 5. Note that as $J_+ = J_-$ exceeds a critical value (around 2.89 for $n = 2$), an island of periodic orbits appears in the phase portrait. This is due to the formation of a local maximum in $2f(\theta)$ and hence, given the asymptotic behaviour $2f(\theta) \sim 4J_+^2 \cos^2 \theta$ as $\theta \rightarrow \pi/2$, due to the formation of a pair of critical points of $2f(\theta)$. These points have a nice geometric interpretation, which we will now describe. First note that

$$\frac{d}{d\theta} 2f(\theta) = 0, \quad f(\theta) = 1 + \frac{f''(\theta)}{2f(\theta)} = 0: \quad (35)$$

Now, the necessary and sufficient condition for \mathbb{M}_n^{eq} to have an isometric immersion as a surface of revolution in \mathbb{R}^3 is that $1 - f(\theta) \geq 0$ for all θ , see [11]. In this case, if we imagine the surface as being generated by rotating a generating curve in the $x_1 x_2$ plane about the x_3 axis (as depicted in figure 4), then $f(\theta) = \cos^2 \theta$, where θ is the angle between the tangent to the generating curve and the x_1 axis. Hence critical points of $2f(\theta)$ are associated with points where the tangent to the generating curve is vertical, and a pair of such points develops precisely when the surface develops a pinched neck. This confirms our visual intuition that the island of closed trajectories appears when the pinched neck forms in \mathbb{M}_n^{eq} .

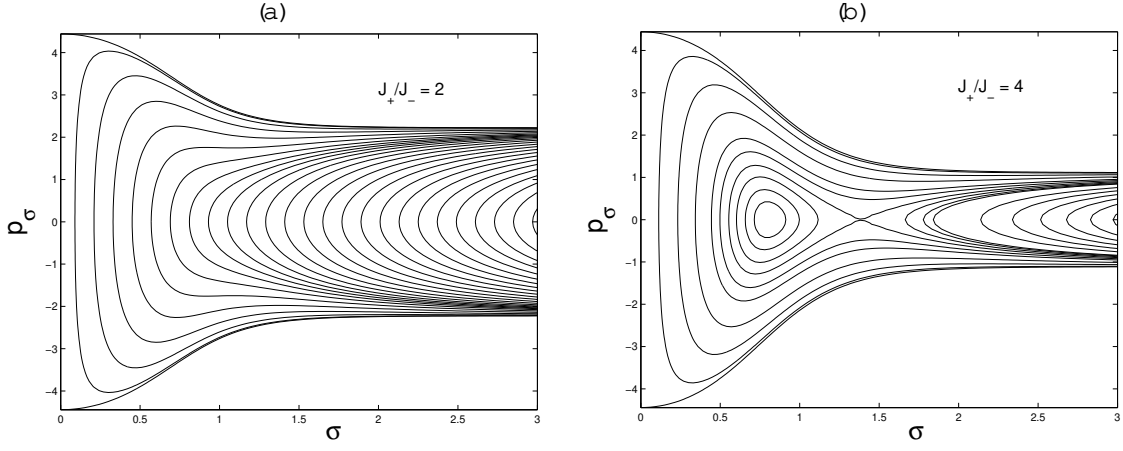


Figure 5: Phase portraits of the geodesic flow in $\mathcal{M}_2^{\text{eq}}$ for (a) $J_+/J_- = 2$ and (b) $J_+/J_- = 4$. Note the island of periodic orbits for the higher value of J_+/J_- .

Recall that the trajectories depicted in figure 5 are the projections of geodesics to the $(\sigma; p_\sigma)$ plane. A closed trajectory in this picture does not necessarily correspond to a periodic geodesic: both the width $\sigma(t)$ and the phase $e^{i\psi(t)}$ are periodic, but with (in general) incommensurate periods. These geodesics are therefore only quasiperiodic, so we call the oscillating n -bubbles associated with them quasibreathers. The time dependence of the width and internal phase of a typical quasibreather is depicted in figure 6. Note that the shape of these solutions really does "breathe". This is in contrast to the internally spinning magnetic solitons (sometimes called breathers) which occur in ferromagnetic spin lattices (with on-site anisotropy), where n_3 has a fixed hump-shaped profile and the spins merely rotate at constant speed about the n_3 axis [12]. For $n = 2$, quasibreathers exist only for $J_+/J_- > 2.89$ (approximately), but for any value of $J_+/J_- > 1$, there is some $n_{\text{min}} \geq 2$ such that the geodesic flow supports quasibreathers of any degree $n \geq n_{\text{min}}$. The dependence of n_{min} on J_+/J_- is shown in figure 7.

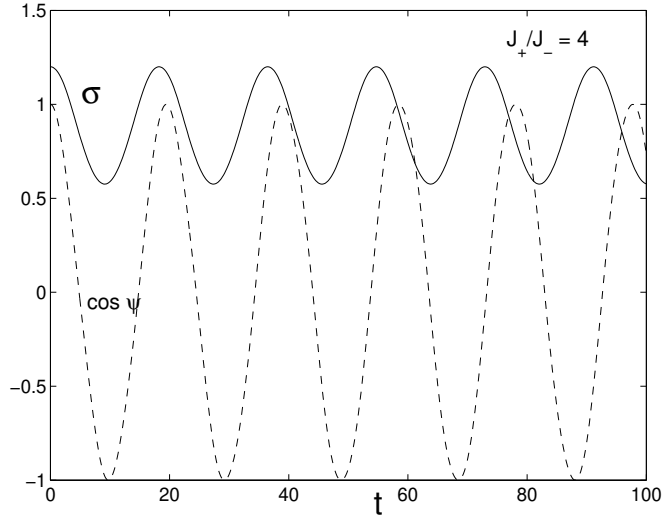


Figure 6: The time dependence of the width σ (solid curve) and internal phase $\cos \psi$ (dashed curve) of a typical degree 2 quasibreather, in a disk inhomogeneity with $J_+/J_- = 4$.

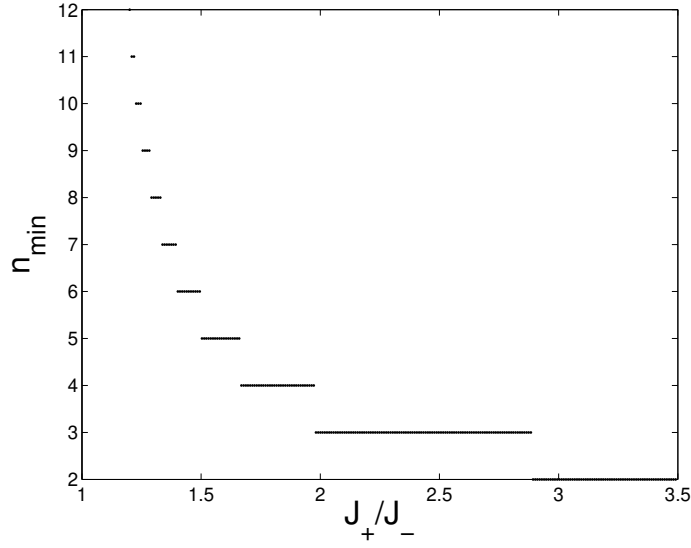


Figure 7: The minimum allowed degree n_{\min} of a quasibreather as a function of the inhomogeneity parameter J_+/J_- .

5 Concluding remarks

We have seen that, in the near continuum regime, a two-dimensional isotropic Heisenberg antiferromagnet with position-dependent exchange integral is described by the relativistic $O(3)$ sigma model on a spatially inhomogeneous spacetime. By conformal invariance, such a model supports static Belavin-Polyakov lumps, which we call bubbles. The trajectories of these bubbles are predicted to behave like light rays propagating in an inhomogeneous medium, with J^{-1} , the inverse exchange integral, identified with the refractive index. In particular, bubbles incident on a straight domain wall are refracted in accordance with Snell's law, and total internal reflection can occur. This refraction phenomenon was noted in [2].

In this paper we have reviewed the analysis of bubble dynamics presented in [2], and extended it beyond the scattering problems previously considered to include the rotationally equivariant dynamics of higher degree bubbles. Here we found that disk J -inhomogeneities with sufficiently large J_+/J_- support quasibreathers: degree $n \geq 2$ bubbles centred in the disk which spin internally while their shape oscillates with a generically incommensurate period.

Our analysis has been conducted entirely within the framework of the geodesic approximation of Manton. The validity of this approximation for the $O(3)$ sigma model remains an open question. In the general context of relativistic field theories of Bogomolny type, it has proved to be very successful at describing soliton scattering processes at low to intermediate energies, where the solitons move essentially as free particles except during a relatively brief interaction phase [9]. The basic domain wall refraction effect seems likely to be a robust feature of the degree 1 bubble dynamics, therefore.

The status of the quasibreather solutions is less straightforward. It is unlikely that the sigma model will support genuine quasiperiodic solutions for any bounded choice of $J(\vec{x})$, because one expects an oscillating, spinning bubble to radiate energy to infinity in the form of small amplitude travelling waves. So the quasiperiodic geodesics in $\mathcal{M}_n^{\text{eq}}$ found here cannot be globally close to the true solutions of the model with the same initial data. One should think of the geodesic approximation as predicting that long-lived oscillating, spinning bubbles exist in the model which are approximately quasiperiodic, but decay over a long time scale.

The only geodesics for which rigorous error estimates have been found are the radial half rays $(t) = vt$ in $\mathcal{M}_n^{\text{eq}}$ for $n \geq 3$ (in the homogeneous case, J constant, though this is unlikely to be crucial). These geodesics describe an equivariant n -bubble collapsing in finite time. Rodnianski and Sterbenz [13] have shown that the actual solutions do indeed collapse in finite time, but that the collapse rate predicted by the geodesic approximation receives a logarithmic correction which becomes significant when the bubble is extremely close

to collapse (i.e. extremely narrow). In the present context, the significance of this deviation is debatable: when the bubble is very narrow, the continuum approximation which led to the sigma model in the first place has presumably already broken down. Indeed, the most important test of the dynamical phenomena predicted here and in [2] is not provided by rigorous analysis of the PDE (2), but by direct numerical simulation of the spin lattice (1) itself. Such simulation is computationally far more intensive than the methods we have used here, and lies beyond the scope of this paper.

Acknowledgements

This paper is based largely on the talk "Magnetic bubble refraction in inhomogeneous antiferromagnets" given by the author at the workshop Nonlinear Physics Theory and Experiment IV, Gallipoli, Italy 2006. His attendance at this workshop was funded by the EPSRC.

References

- [1] F.D.M. Haldane, "Continuum dynamics of the 1-D Heisenberg antiferromagnet: identification with the O(3) nonlinear sigma model" Phys. Lett. 93A (1983) 464.
- [2] J.M. Speight, "Sigma models on curved space and bubble refraction in doped antiferromagnets" Nonlinearity 19 (2006) 1565.
- [3] S. Konineas and N. Papanicolaou, "Vortex dynamics in 2D antiferromagnets" Nonlinearity 11 (1998) 265.
- [4] A.A. Belavin and A.M. Polyakov, "Metastable states of two-dimensional isotropic ferromagnets" JETP Lett. 22 (1975) 245.
- [5] N.S. Manton, "A remark on the scattering of BPS monopoles" Phys. Lett. 110B (1982) 54.
- [6] R.S. Ward, "Slowly moving lumps in the CP^1 model in $(2+1)$ dimensions" Phys. Lett. 158B (1985) 424.
- [7] R.A. Leese, "Low energy scattering of solitons in the CP^1 model" Nucl. Phys. B 344 (1990) 33.
- [8] P.J. Ruback, "Vortex string motion in the abelian Higgs model" Nucl. Phys. B 296 (1988) 669.
- [9] N.S. Manton and P.M. Sutcliffe, Topological Solitons, Cambridge University Press, Cambridge, UK, (2004) pp 102-108.
- [10] J.M. Speight, "Low energy dynamics of a CP^1 lump on the sphere" J. Math. Phys. 36 (1995) 796.
- [11] J.A. McGlade and J.M. Speight, "Slow equivariant lump dynamics on the two sphere" Nonlinearity 19 (2006) 441.
- [12] A.M. Kosevich, B.A. Ivanov and A.S. Kovalev, "Magnetic solitons" Phys. Rep. 194 (1990) 117.
- [13] I. Rodnianski and J. Sterbenz, "On the formation of singularities in the critical O(3) sigma model" preprint math.AP/0605023 (2006)